Measurement and Analysis of Ion Distribution in Laminar Flame Using an Electrostatic Probe

Young Han Kim† and Jang Ho Seo

Dept. of Chemical Engineering, Dong-A University, Busan 604-714, Korea
(*Received 3 August 2001 • accepted 24 September 2001*)

Abstract−An electrostatic probe is utilized to determine the ion distribution in a laminar flame. The probe is developed to be implemented in the ion measurement of combustion process contained in a solid container, and therefore the probe fabrication and the construction of a whole measurement system are explained in detail. Also, a numerical analysis is conducted to compare experimental measurement with the computed temperature and concentration. The ion distribution of four different flames of various fuel/air ratios is measured to analyze the distribution for understanding the combustion process. An explicit method is implemented to solve a set of partial differential equations of material and energy balances. Comparison between the measured distribution and the computed distribution of temperature indicates that the ion formation is closely related to the temperature distribution.

Key words: Electrostatic Probe, Laminar Flame, Ion Concentration, Combustion, Numerical Analysis

INTRODUCTION

The analysis of combustion processes is difficult, because fast and complex reactions are involved in the process. Moreover, its highly exothermic reaction makes the measurement of composition and temperature in a flame complicated. For the increased efficiency of the combustion process, various catalysts can be utilized to reduce the emission of un-reacted fuel [Kirchnerova, 1999; Cho et al., 1999; Chaouki et al., 1999].

There are two methods for measuring such a fast process: electrical and optical techniques. Both of them are suitable for fast varying systems. Though recently developed laser measurement techniques [Bengtsson, 1996; Choudhuri and Gollahalli, 2000; Yujing and Mellouki, 2001] scan a whole cross-section at one time and provide information without spatial limitation, the condition of a measurement chamber has to be adequate for the optical measurement. On top of the high cost of measurement instruments, a technique requiring optical path is not applicable to a combustion system having steel walls; most combustion chambers in practice are made of steel. Spectroscopy was implemented to monitor the concentration of OH radical during soot oxidation [Furukawa et al., 1994, 1998], but its application is also limited like laser measurement techniques. The optical technique was also utilized in the radical measurement of low oxygen air combustion [Chung et al., 1999].

An electrostatic measurement system is simple and inexpensive to implement in flame analysis. It detects only a local composition in the flame, but a new data acquisition system connected to a personal computer getting multiple measurements [Waterfall et al., 1996] at the same moment solves the problem of spatially limited detection. Ion measurement in a laminar flame was conducted by Shcherbakov et al. [1988], and in turbulent flames Furukawa et al. [1994, 1998] measured the flame using an electrostatic probe. Also, numerical analysis of the turbulent flame was conducted by McKentry

et al. [1999] and Choi et al. [2001].

In this study, an electrostatic probe system for the ion measurement in a flame is developed and utilized in a butane-air system. The fabrication detail of the measurement system is explained for the researcher being expected to utilize the probe. Also, a numerical calculation using a set of partial differential equations of mass and energy balances is conducted to compare with the experimental measurement.

NUMERICAL ANALYSIS

A detailed description of the burner used in this study is given in Fig. 1. Half-inch size fittings are utilized to assemble a burner. As
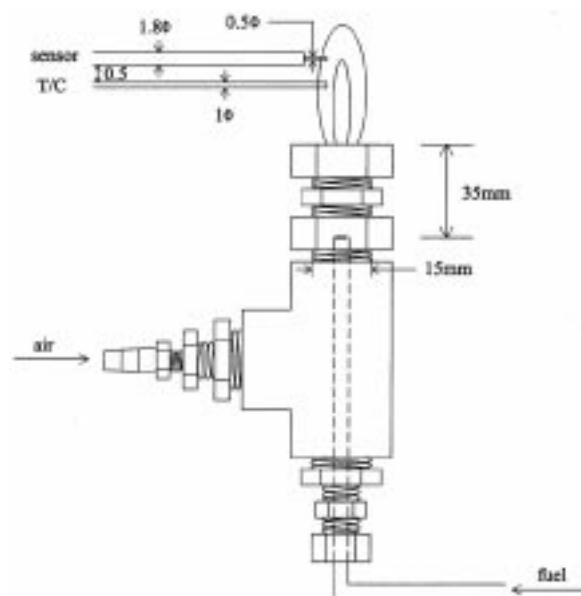

Fig. 1. Schematic diagram of electrostatic probe, T/C thermometer, and burner.

†To whom correspondence should be addressed.
E-mail: yhkim@mail.donga.ac.kr

fuel of the burner n-butane gas is provided through 1/8 inch tubing installed in the center of the burner, air is separately fed for the combustion.

For the simplicity of the computation, some assumptions are made in the development of system equations. Because gas is supplied as a laminar flow in vertical direction, no significant radial gas flow is expected and radial transport of mass and energy is dominated by diffusion. In addition, axial gas flow is large enough to ignore axial diffusion, and the flow is steady and constant.

With the assumptions, a material balance in steady state is formulated as

$$v_z \frac{\partial c}{\partial z} = D \frac{1}{r} \frac{\partial}{\partial r} \left[r \frac{\partial c}{\partial r} \right] - r_A \tag{1}$$

B.C. $\frac{\partial c}{\partial r} = 0$ at $r = 0$

$c = 0$ at $r = R$

$c = c_0$ at $z = 0$, $r = 0$

$c = 0$ at $z = 0$, $r > 0$

and an energy balance is

$$\rho C_p v_z \frac{\partial T}{\partial z} = k_c \frac{1}{r} \frac{\partial}{\partial r} \left[r \frac{\partial c}{\partial r} \right] + (-\Delta H_r) r_A \tag{2}$$

B.C. $\frac{\partial T}{\partial r} = 0$ at $r = 0$

$\frac{\partial T}{\partial r} = 0$ at $r = R$

$T = T_0$ at $z = 0$

The chemical reaction mechanism of a combustion process is very complicated. Because the approximate composition and temperature profiles are studied here, a first order simple reaction mechanism is utilized in the analysis.

The material balance in dimensionless form is

$$\frac{\partial c'}{\partial z'} = \frac{LD}{R^2 v_z} \frac{1}{r'} \frac{\partial}{\partial r'} \left[r' \frac{\partial c'}{\partial r'} \right] - \frac{kL}{v_z} c' \tag{3}$$

where the primes indicate the dimensionless variables as below.

$c' = \frac{c}{c_0}$,

$z' = \frac{z}{L}$,

and

$r' = \frac{r}{R}$

And the energy balance is

$$\frac{\partial T'}{\partial z'} = \frac{k_c}{\rho C_p R^2 v_z} \frac{\partial}{\partial r} \left[r \frac{\partial T'}{\partial r} \right] + \frac{(-\Delta H_r) c_0}{\rho C_p (T_m - T_0)} \frac{kL}{v_z} c' \tag{4}$$

where

$T' = \frac{T - T_0}{T_m - T_0}$

Though the system is described in cylindrical coordinates, a two-dimensional rectangular grid containing the center axis is used in

Table 1. Parameters for numerical calculation

Symbol	Value
L	4 cm
D	0.225 cm^2/s
R	1 cm
v_z	21.2 cm/s
k_c	1.2×10^{-5} cal/(cm ºC s)
E_A	1.25×10^5 J/mol
T_m	1,000 ºC
T_0	256 ºC
c_0	1×10^{-3} g/cm^3
r	1.16×10^{-3} g/cm^3
C_p	0.272 cal/g ºC
$-\Delta H_r$	1.09×10^4 cal/g

the formulation of the finite difference equations from Eqs. (3) and (4). An explicit technique is implemented here to solve the set of parabolic partial differential equations. The concentration and temperature are simultaneously found at the same axial position. The grid sizes in radial and axial directions are determined to satisfy the stability criterion [Constantinides and Mostoufi, 1999].

The average size of flame is 2 cm in radius, and the axial velocity obtained is an air flow rate of 4 liters per minute. Fuel flow is too small to be included. Physical properties are taken from those of air. Kinetic information is from a reference [Librovich, 1999]. Table 1 lists the parameters used in this study.

EXPERIMENTAL

1. Preparation of Probe

Because the electrostatic probe is expected to be utilized in a concealed solid container and to measure a local ion concentration, it is made of a small stainless steel tube with a thin platinum wire. The tip of the wire is extruded by 1 mm from the end of the protective tube. Fig. 1 shows the detailed dimensions of the probe. The wire is installed inside the tube, and the wire is insulated from the tube for the measurement of electric current between them during the measurement of ion concentration. An electric circuit described in Fig. 2(a) is used for the current determination. The voltage measurement across the resistor gives the current. The dc voltage is supplied from the circuit in Fig. 2(b), of which the positive electrode is connected to the center wire and the negative is to the protective tube. For the high voltage supply, the circuit is built with high voltage components. The signal voltage is directly provided to a home-made A/D converter described in Fig. 3. The digitized measurement from the A/D converter is transferred to a PC through a printer data port. To eliminate noise contained in the signal, an integration type A/D converter is used, though its conversion time is longer than that of successive approximation type. The sampling frequency of the home-made converter is 10 Hz, which is high enough for the experiment. Three signals of ion current, temperature, and probe position are separately and sequentially transferred to the A/D converter. The control of the input signal transfer is conducted through a PC. The converter generates four digits of binary coded decimal data that are sent to the PC through a parallel port. The conversion
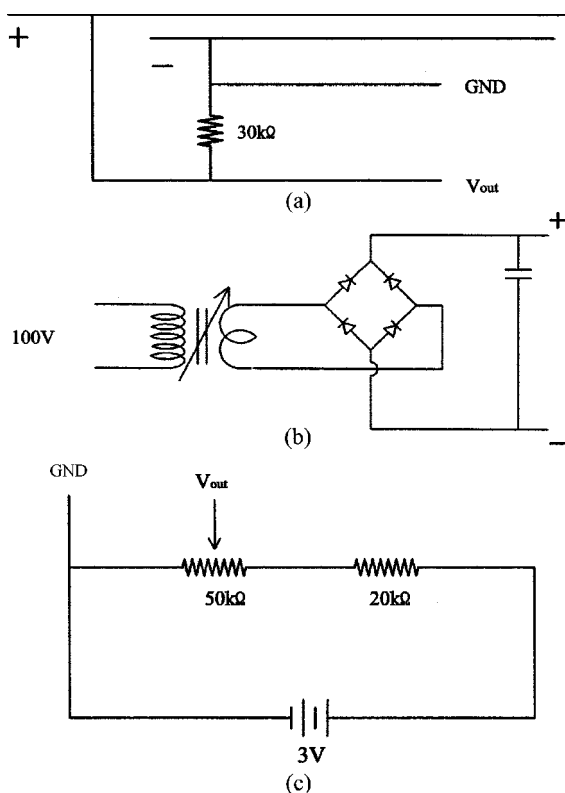
Fig. 2. Circuit diagrams of probe current detection (a), dc power supply (b), and position detection (c).
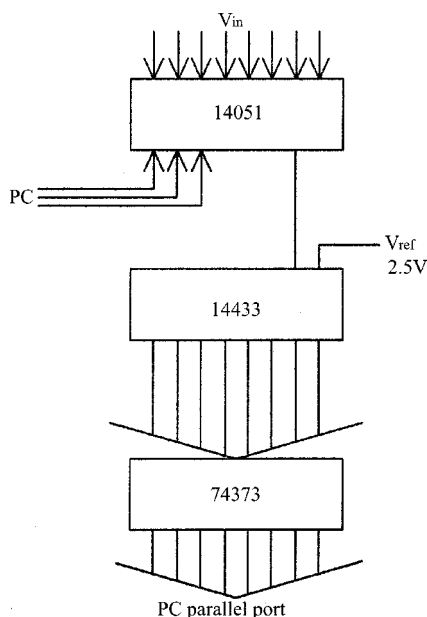

Fig. 3. Schematic diagram of a home-made analog-to-digital converter.

of the data is included in the program for the experiment.

The amount of electric current is proportionally related to the ion concentration, but the detection of weak current signal is impossible without applying external voltage supply. The voltage and current have a linear relation within a certain range [Burtscher et al., 1990]. Low voltage gives better ion measurement as long as the
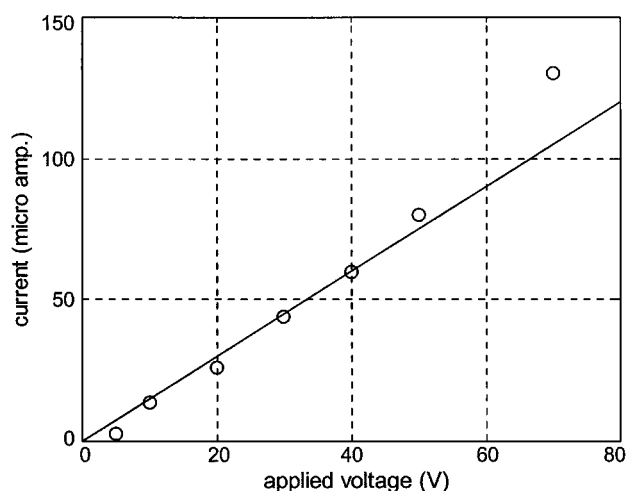
Fig. 4. Relation between dc power supply and probe current.

current signal is detected. The relation between the voltage and measured current is shown in Fig. 4. A linear relation is observed up to 40 volts, and therefore 20 volts are applied in this experiment after the sensitivity and linearity between the supply voltage and current signal.

For the measurement of temperature a thermocouple thermometer of K type is utilized here. Thermocouple selection is explained in Heitor and Moreira [1993]. A temperature indicator (Konics Co., Korea, Model KN-2200) is installed for the monitoring and data transfer to a PC. The indicator generates 4-20 ma current output, and it is converted to voltage signal by using a 100 ohm resistor directly connected to the output port. The voltage signal is fed to the A/D converter. For the calibration of the thermometer, temperature and measured voltage are plotted in Fig. 5, which indicates a good linear relation.

In order to adjust the position of a probe and a T/C thermometer, a driving system is constructed as given in Fig. 6. The set of the probe and thermometer moves forward and backward by driving a geared induction motor of which the shaft is coupled with a screw. The motor turns both directions. The turning of the screw pushes or pulls a probe bracket. The location of the bracket is detected from
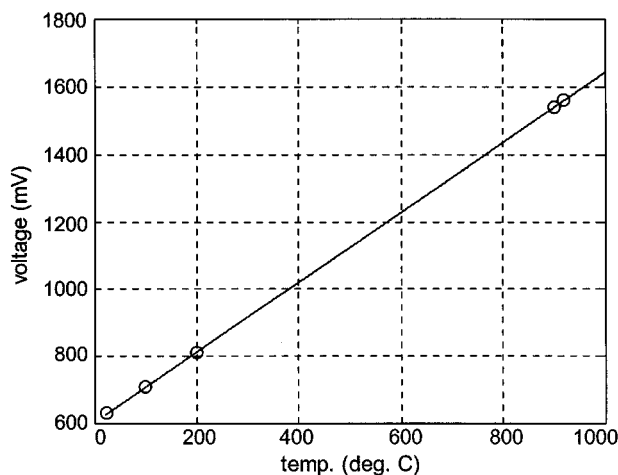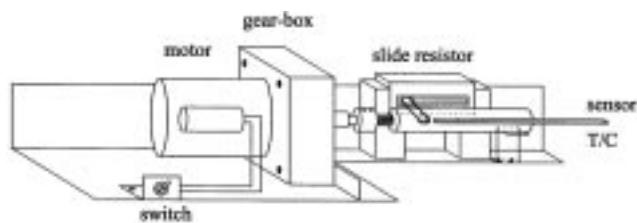

Fig. 5. Calibration of temperature measurement.

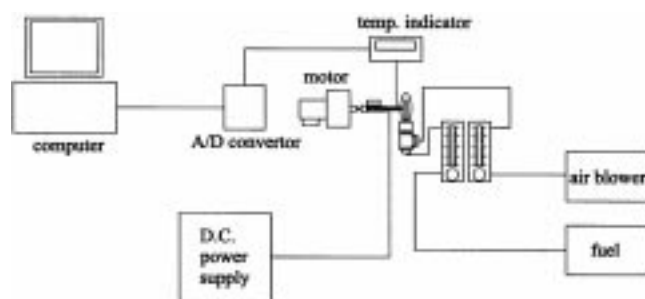Fig. 6. Schematic diagram of probe positioning system.
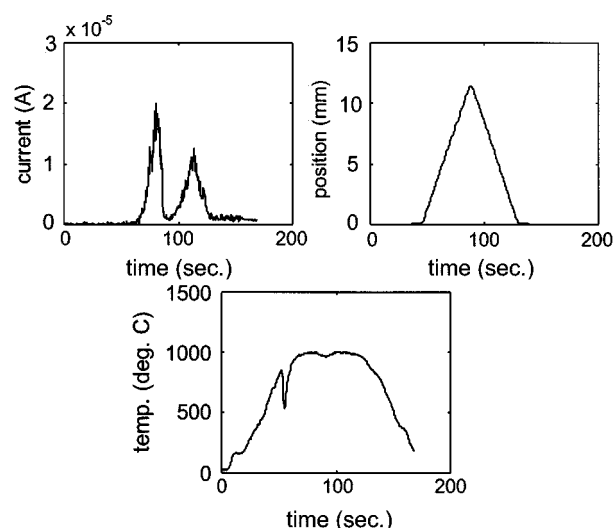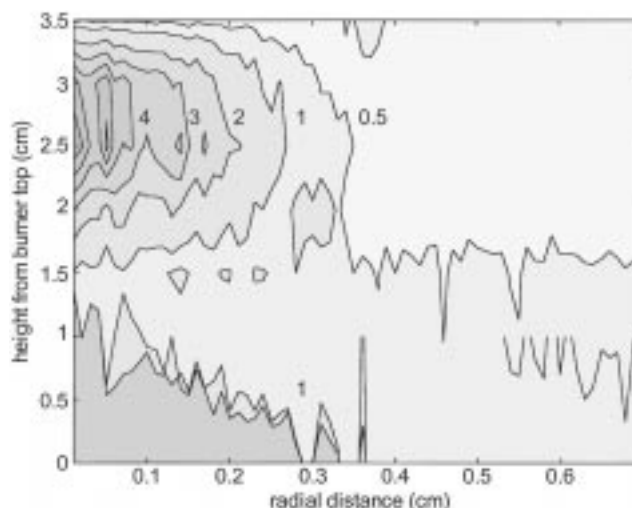

Fig. 7. Schematic of experimental setup.

Fig. 8. Measurement of current, probe position, and temperature.

Fig. 9. Distribution of current measurement in microamperes for fuel supply of 30 cm³/minute.

a slide resistor connected to the bracket. The circuit demonstrated in Fig. 2(c) is implemented to measure the position as a voltage signal. The voltage is measured through the A/D converter.

2. Burner Construction

For the simple assembly of a burner, half-inch fittings are utilized. Fuel is supplied through a 1/8 inch copper tube installed at the center of the burner. The detailed dimension of the burner is given in Fig. 1. Air is supplied from the side of the burner.

3. Experimental Setup

The whole arrangement of experimental equipment is shown in Fig. 7. Air is provided from an air blower and a rotameter for the flow measurement. Flow rate is adjusted by using a needle valve attached on the rotameter. Fuel is drawn from a cylinder and is supplied by the same manner as for the air supply. The probe signal, signal from temperature indicator, and probe position voltage are directed to the A/D converter. The digitized measurement is provided to the PC, and the data are stored in the PC for the analysis later.

4. Experimental Procedure

The probe set is positioned at a given height from the top of burner head. The height is set from 0.5 cm, and is increased by 0.5 cm until no current is detected. The air blower is activated for the air supply, and the needle valve on the rotameter is adjusted for a given flow rate. Then fuel is supplied at a desired flow rate. Gas of n-butane is used as the fuel. After a couple of seconds, the flame is ignited. While the computer program for data collection is running, the probe driving motor is activated for forward scanning until the probe passes all the way through the flame and for backward scanning. After the probe returns to its initial position, the program stops and the flame extinguishes.

RESULTS AND DISCUSSION

In order to examine the experimental setup performance, a test run is conducted and the result is shown in Fig. 8. While the probe is moving forward and backward as shown in the figure of position, electric current and temperature are measured and displayed in the two left figures. Because of high convective heat transfer near the flame and conduction through the protective tube, an accurate measurement of point temperature is not available as noticed from the broad temperature distribution. Note that a thin thermometer of 1 mm in diameter is utilized here. Therefore, the flame analysis is conducted by examining the current variation only.

When fuel is supplied at the rate of 30 cm³/min., the ion distribution is given in Fig. 9. The numbers in the figure indicate the amount of current in microampere units. A circular pattern is observed at the height of 2.5 cm, and weak signal is detected at bottom. A similar pattern of current measurement is found with the rate of 40 cm³/min. as shown in Fig. 10, but the strength of the current is twice as much as the previous one. With the rates of 50 and 60 cm³/min, almost identical current distribution is obtained and described in Figs. 11 and 12. About 5 times as high current as the last one is detected in these cases. And the current distribution in the last two cases is
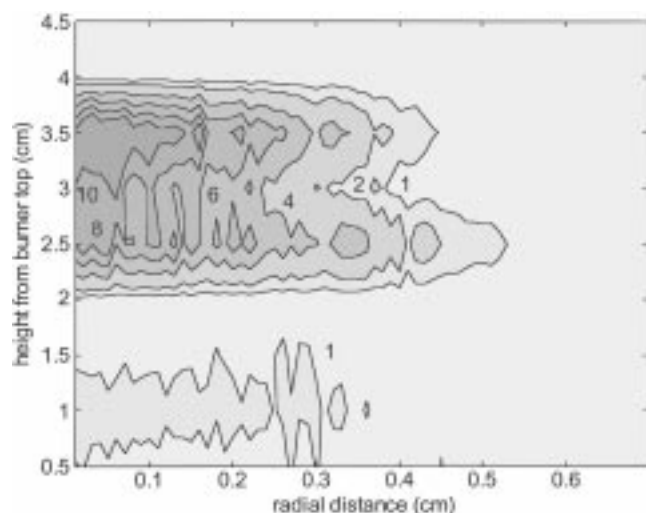
Fig. 10. Distribution of current measurement in microamperes for fuel supply of 40 cm³/minute.
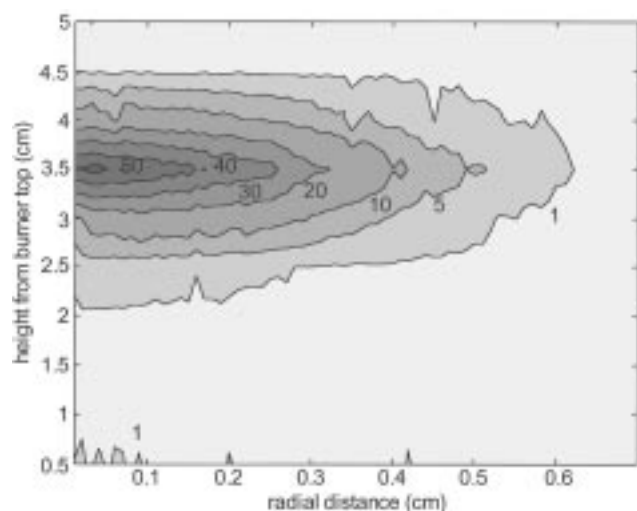

Fig. 11. Distribution of current measurement in microamperes for fuel supply of 50 cm³/minute.
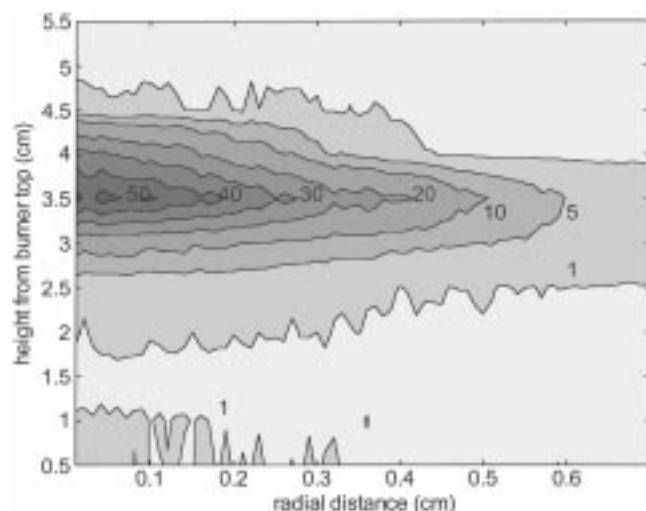

Fig. 12. Distribution of current measurement in microamperes for fuel supply of 60 cm³/minute.

almost identical except flame length is a little longer. With a small amount of fuel supply, the ion generation is limited from the amount of the fuel. When the supply is high enough, the current strength is saturated owing to the air supply. The measurement of ion distribution gives the optimum fuel and air ratio. From the measurements of this study it is observed that the fuel flow rate of 50 cm³/min is optimum because the rate gives the highest ion concentration, meaning complete combustion and the maximum generation of heat. Being less than the flow rate implies excessive air supply, and higher fuel flow produces incomplete combustion.

For a typical case of a laminar flame, fuel concentration and temperature distributions are calculated from the procedure explained in the section of numerical analysis. The parameters listed in Table 1 for the computation of concentration and temperature are from the case of experimental results shown in Fig. 9. Fig. 13 shows the fuel concentration distribution in dimensionless position of the flame.
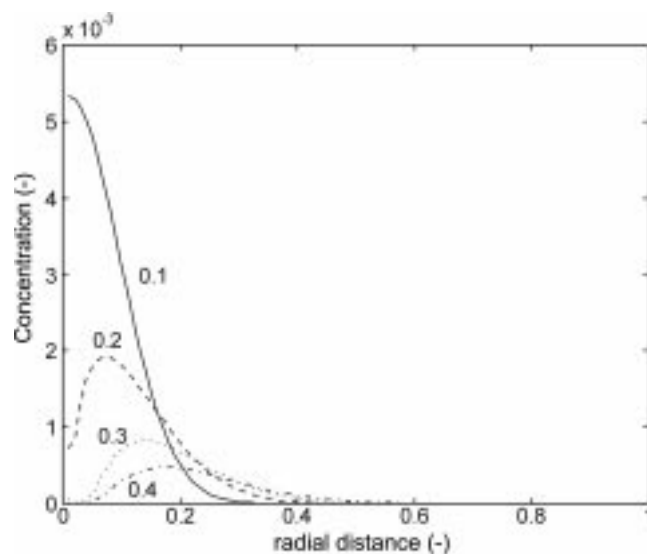

Fig. 13. Calculated distribution of dimensionless fuel concentration (Numbers on the curves are dimensionless axial distance).
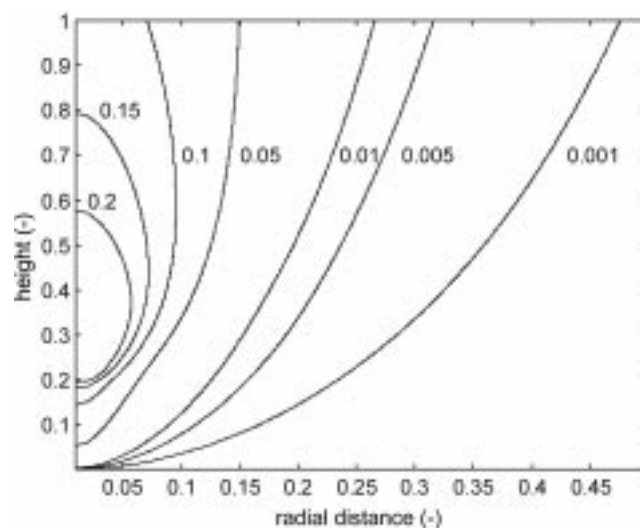

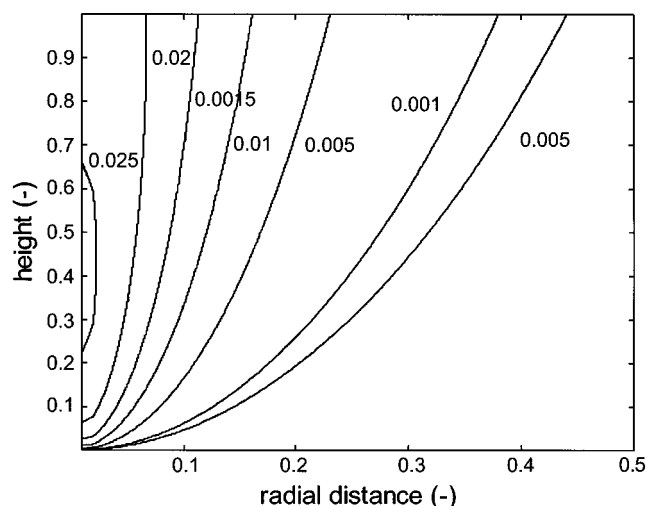**Fig. 14. Calculated distribution of dimensionless temperature.**

Fig. 15. Calculated distribution of dimensionless temperature with increased gas velocity.

The numbers given on the curves are dimensionless concentrations. Because fuel burns from outside of the flame, high concentration is observed in the center and the concentration decreases as flame goes up. Temperature distribution is given in Fig. 14. Again, the numbers on the curves are dimensionless temperatures. The highest temperature is observed at the center and one-third of axial location. The temperature diminishes as moving away from the center. Though the location of the highest temperature is different from the current measurement of the experiment, the patterns of both distributions of ion from the experiment and temperature from the numerical calculation are similar. Despite the fact that complex chemical reactions are involved in combustion process, high temperature indicates high rate of exothermic reaction and ion generation. This explains the similarity of the temperature and ion concentration distributions. The difference in location of the center of circular pattern is from the discrepancy in parameters used in the numerical calculation and the experiment. The gas flow rate in the numerical computation is determined from the supplied air flow rate, but secondary air supply from the surrounding of flame is significant in the actual experiment. Including the secondary supply to the flow to increase the flow rate by 50% moves the center upward as shown in the difference between Figs. 14 and 15. This is an example to explain the discrepancy in some of the parameters used in the simulation.

The circular patterns below the center are similar in the distributions of calculated temperature and measured ion concentration, but those above the center are quite different. While the high concentration ions are consumed by reaction and are not detected above the center, the heat generated from reaction moves upward to be sensed as shown in the distribution.

Because the distribution of ions explains the combustion process the best, many studies dealing with combustion pursue an efficient means to measure the distribution. For example, the combustion process in an internal engine for an automobile is directly related to the efficiency of the engine. The confined structure of the engine prevents optical measurement of the ions, and therefore atechnique utilizing an electrostatic probe is useful to such an application. It is simple to fabricate and is also inexpensive compared with laser instruments.

CONCLUSION

The measurement of ion concentration in a laminar flame is conducted by utilizing an electrostatic probe, which is designed for the detection of ion distribution in a confined combustion chamber. The details of probe fabrication and experimental setup are provided here. In addition, a numerical analysis is carried out to compare the computed distribution of concentration and temperature with the experimental outcome.

The distribution of ion in the flames is measured with different fuel supply rates. The analysis of the distributions gives the optimum ratio of fuel and air supply. Also, the result of the numerical temperature calculation shows a similar pattern with the ion distribution measured experimentally. In other words, either measurement of temperature or ion distribution gives identical information for the analysis of a flame.

ACKNOWLEDGMENT

NOMENCLATURE

c : concentration [g/cm^3]
c_0 : initial concentration [g/cm^3]
C_p : heat capacity [cal/g $^\circ$C]
D : diffusivity [cm^2/s]
E_A : activation energy [J/mol]
$-\Delta H_r$: heat of reaction [cal/g]
k : reaction rate constant [1/s]
k_c : thermal conductivity [cal/(cm $^\circ$C s)]
k_0 : collision constant [1/s]
L : flame length [cm]
R : flame radius [cm]
r : radius [cm]
r_A : rate of reaction [g/cm^3 s]
T : temperature [$^\circ$C]
T_m : maximum temperature [$^\circ$C]
T_0 : initial temperature [$^\circ$C]
v_z : axial linear velocity [cm/s]
z : axial distance [cm]

Greek Letter

ρ : density [g/cm^3]

REFERENCES

Bengtsson, P.-E., "Simultaneous Two-Dimensional Visualization of Soot and OH in Flames using Laser-Induced Fluorescence," *Appl. Spectroscopy*, **50**, 1182 (1996).

Burtscher, H., Glinz, A. and Ochs, M., "Ions in Combustion Exhaust as Soot Monitor," *J. Aerosol Sci.*, **21**, S579 (1990).

Chaouki, J., Klvana, D. and Guy, C., "Selective and Complete Catalytic

Oxidation of Natural Gas in Turbulent Fluidized Beds," *Korean J. Chem. Eng*., **16**, 494 (1999).

Cho, S. J., Ryoo, M. W., Song, K. S., Lee, J. H. and Kang, S. K., "A Catalytic Combustion Technology of Concentrated VOCs in Textile Coating Process," *Korean J. Chem. Eng*., **16**, 478 (1999).

Choi, Y. C., Li, X. Y., Park, T. J., Kim, J. H. and Lee, J. G., "Numerical Analysis of the Flow Field inside an Entrained-Flow Gasifier," *Korean J. Chem. Eng*., **18**, 376 (2001).

Choudhuri, A. R. and Gollahalli, S. R., "Laser Induced Fluorescence Measurements of Radical Concentrations in Hydrogen-Hydrocarbon Hybrid Gas Fuel Flames," *Int. J. Hydrogen Energy*, **25**, 1119 (2000).

Chung, D. H., Yang, J. B., Noh, D. S. and Kim, W. B., "An Experimental Study on High Temperature and Low Oxygen Air Combustion," *Korean J. Chem. Eng*., **16**, 489 (1999).

Constantinides, A. and Mostoufi, N., "Numerical Methods for Chemical Engineers with MATLAB Applications," Prentice Hall PTR, New Jersey, 396 (1999).

Furukawa, J., Nakamura, T. and Hirano, T., "Electrostatic Probe Measurement to Explore Local Configuration of a High Intensity Turbulent Premixed Flame," *Combust. Sci. and Tech*., **96**, 169 (1994).

Furukawa, J., Hirano, T. and Williams, F. A., "Burning Velocities in a Turbulent Premixed Flame," *Combust. and Flame*, **113**, 487 (1998).

Harano, A., Sadakata, M. and Sato, M., "Soot Oxidation in a Silent Discharge," *J. Chem. Eng*., *Japan*, **24**, 100 (1991).

Harano, A., Murata, K., Takamizawa, K. and Sadakata, M., "Oxidation of Carbonaceous Particles in Silent Discharge Reactor," *J. Chem. Eng., Japan*, **31**, 700 (1998).

Heitor, M. V. and Moreira, A. L. N., "Thermocouples and Sample Probes for Combustion Studies," *Prog. Energy Combust. Sci*., **19**, 259 (1993).

Kirchnerova, J., "Materials for Catalytic Gas Combustion," *Korean J. Chem. Eng*., **16**, 427 (1999).

Librovich, B. V., Makhviladze, G. M., Roberts, J. P. and Yakush, S. E., "Numerical Analysis of Laminar Combustion of Fuel Gas Clouds," *Combust. and Flame*, **118**, 669 (1999).

McKenty, F., Gravel, L. and Camarero, R., "Numerical Simulation of Industrial Boilers," *Korean J. Chem. Eng*., **16**, 482 (1999).

Shcherbakov, N. D., Ospanov, B. S. and Fialkov, B. S., "Negative Ion Distribution in Hydrocarbon Flames," *Combust. Explos. Shock Waves*, **24**, 313 (1988).

Waterfall, R. C., He, R., White, N. B. and Beck, C. M., "Combustion Imaging from Electrical Impedance Measurements," *Meas. Sci. Technol*., **7**, 369 (1996).

Yujing, M. and Mellouki, A., "Temperature Dependence for the Rate Constants of the Reaction of OH Radicals with Selected Alcohols," *Chem. Phys. Letters*, **333**, 63 (2001).